Computer Modeling in Engineering & Sciences CMES, vol.122, no.2, pp.661-674, 2020

Stress Analysis of Printed Circuit Board with Different Thickness and Composite Materials Under Shock Loading

Kuan-Ting Liu[1], Chun-Lin Lu[1], Nyan-Hwa Tai[2] and Meng-Kao Yeh[1, *]

Abstract: In this study, the deformation and stress distribution of printed circuit board (PCB) with different thickness and composite materials under a shock loading were analyzed by the finite element analysis. The standard 8-layer PCB subjected to a shock loading 1500 g was evaluated first. Moreover, the finite element models of the PCB with different thickness by stacking various number of layers were discussed. In addition to changing thickness, the core material of PCB was replaced from woven E-glass/epoxy to woven carbon fiber/epoxy for structural enhancement. The non-linear material property of copper foil was considered in the analysis. The results indicated that a thicker PCB has lower stress in the copper foil in PCBs under the shock loading. The stress difference between the thicker PCB (2.6 mm) and thinner PCB (0.6 mm) is around 5%. Using woven carbon fiber/epoxy as core material could lower the stress of copper foil around 6.6% under the shock loading 1500 g for the PCB with 0.6 mm thickness. On the other hand, the stress level is under the failure strength of PCBs with carbon fiber/epoxy core layers and thickness 2.6 mm when the peak acceleration changes from 1500 g to 5000 g. This study could provide a reference for the design and proper applications of the PCB with different thickness and composite materials.

Keywords: Stress analysis, printed circuit board, composite material, finite element analysis, shock loading.

1 Introduction

Printed circuit board (PCB) is an important part to connect active and passive components for current electronic devices. Therein, electronic circuits in PCB and the components form a conductive connection during the operation of devices [Wang (2012)]. A good PCB design could provide a stable working environment for communication between components. Three major types of PCB are used in current industry for various considerations, including the single-sided PCB, double-sided PCB and multilayer PCB [Ebnesajjad (2013)]. The single-sided PCB has the advantage of lower cost, but the capacity of mounting components is limited due to single-side usage only. The double-sided PCB has two conductive pads on top and bottom sides for mounted components

[1] Department of Power Mechanical Engineering, National Tsing Hua University, Hsinchu, 30013, Taiwan.

[2] Department of Materials Science and Engineering, National Tsing Hua University, Hsinchu, 30013, Taiwan.

[*] Corresponding Author: Meng-Kao Yeh. Email: mkyeh@pme.nthu.edu.tw.

Received: 28 June 2019; Accepted: 14 August 2019.

and connection of two sides by via. Compared with the single-sided PCB, the double-sided PCB could save more area to make a package compact. For more complex electronic circuit design, the multilayer PCB is chosen for the package with smaller space. Conductive and insulating layers are sandwiched to form the multi-layer PCB [Tummala (2001)]. The number of layers in the PCB as motherboard of electronic devices depends on its requirements. The PCB with four to eight layers is common in the industry. The PCB consists of dielectric substrates and conductors; and the copper foil is a general material as the conductor because of its low rate of surface oxidation and compatibility of substrates [Grout (2008); Hanafi, Jobiliong, Christiani et al. (2012)]. FR-4, a composite material of woven fiberglass cloth and epoxy resin binder, is the most popular material used as substrate of PCB since it is versatile, including electrical insulation with high dielectric strength, high strength-to-weight ratio, moisture resistance, and relative temperature resistance [Nanotech Elektronik (2019)]. Therefore, a lot of portable products adopt FR-4 PCB as the motherboard.

Many situations might induce failure of PCB, including circuit failure due to improper component design, environmental factors and operation. These environmental factors, such as temperature and moisture, cause delamination between layers and material crack inside the PCB. Some literatures investigated the effect of these factors, including studying the temperature effect by thermal cycling [Zhang, Ding and Sheng (2009); Zhang, Liu, Wang et al. (2015)]. On the other hand, the impact drop test for PCB is quite important before mass production for the development of PCB, especially for application of portable products. Reiff et al. [Reiff and Bradley (2005)] evaluated the lead-free ball grid array (BGA) solder joint reliability by a mechanical shock test and identified the failure of BGA by the strain rate. Wang et al. [Wang, Low, Che et al. (2003)] performed the simulation of the PCB drop test and focused on the displacement and acceleration of the PCB during the drop test. Ong et al. [Ong, Shim, Chai et al. (2003)] indicated the bias between the product-level and board-level drop impact test by comparing the mechanical responses of PCBs. Wong et al. [Wong, Lim, Lee et al. (2002)] studied the mechanics and physics of the board-level drop test to provide the fundamental understanding for PCB and interconnection design. They found geometrical stress concentration is critical in the impact of strength of the interconnections. Jie et al. [Jie, Lim and Tay (2004)] performed the dynamic drop impact test by the finite element analysis and predicted the critical failure location by the bending curvature of PCB.

In this paper, the deformation and stress distribution of the PCB during the mechanical shock test were investigated. Various PCB models with different thickness and composite materials were used to discuss the strength of PCB during the shock loading by the finite element analysis.

2 Finite element analysis

The commercial finite element software ANSYS [ANSYS (2009)] was used to build the finite element models of the PCB and to perform the dynamic analysis by giving the PCB an acceleration loading in this study. The deformation and stress distribution in the PCB were discussed, after the models were subjected to an external load by referring to the industry criteria [Integrated Service Technology (2019)]. In addition, the PCBs with

different thickness and composite materials were also evaluated.

2.1 Finite element models

According to the JEDEC standard for board level drop test, JESD22-B111 [JESD22 B111 (2003)], the length and width of the PCB in this study are 132 mm and 77 mm respectively, as shown in Fig. 1. Two different stacking structures were built. One is a standard 8-layer stacked PCB, which consists of 8 layers of copper foil and 7 layers of woven E-glass/epoxy, and a total thickness of 1.6 mm [Pcbcart (2019)], as shown in Fig. 2. For considering the strength of the PCB with different thickness, the other stacking structure of the PCB with different thickness of E-glass/epoxy and copper foil layers was adopted from literature [Wang, Low, Pang et al. (2006)], as shown in Fig. 3. Therein, the thickness of each E-glass/epoxy layer is 0.178 mm and inner and outer copper foil are 0.0178 mm and 0.035 mm respectively.

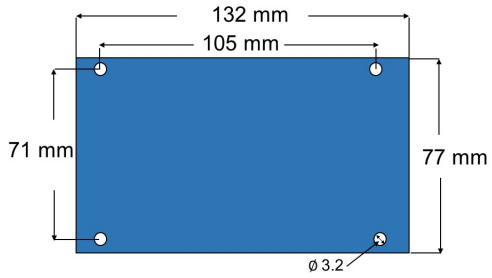

Figure 1: Schematic of PCB

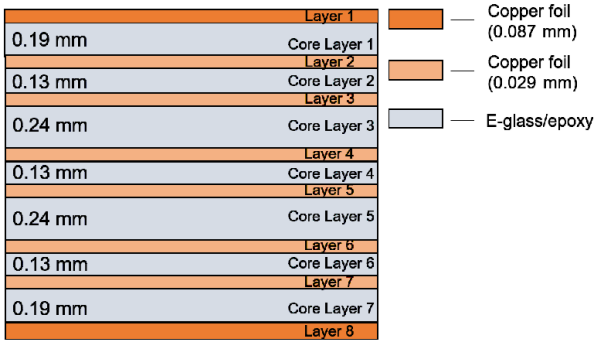

Figure 2: Schematic of standard 8-layer PCB

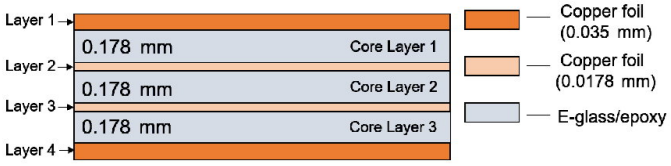

Figure 3: Schematic of finite element model of PCB with different thickness

The material properties of woven E-glass/epoxy composites used in finite element models are shown in Tab. 1 [Tan, Tong and Steven (2001); Rahman, Rangari and Jeelani (2015)]. The non-linear material property of copper foil was considered in the analysis, as shown in Tab. 2 [Iannuzzelli (1991)]. Except the finite element model of the PCB with woven E-glass/epoxy composites, the PCB model with woven carbon fiber/epoxy composites was also analyzed. Tab. 3 shows the material properties of woven carbon fiber/epoxy composites [Qrimli, Mahdi and Ismail (2015); Performance Composites (2009)].

Table 1: The material properties of woven E-glass/epoxy composites [Tan, Tong and Steven (2001); Rahman, Rangari and Jeelani (2015)]

Young's modulus		Shear modulus		Poisson ratio		Density
E_x (GPa)	29.46	G_{xy} (GPa)	5.3987	ν_{xy}	0.1329	
E_y (GPa)	28.03	G_{yz} (GPa)	4.1740	ν_{yz}	0.3000	2000 kg/m^3
E_z (GPa)	12.85	G_{xz} (GPa)	4.1212	ν_{xz}	0.3180	

Table 2: The material property of copper foil [Iannuzzelli (1991)]

Strain	Stress	Poisson ratio	Density
0.001	120 MPa		
0.004	186 MPa		
0.01	217 MPa	0.3	8930 kg/m^3
0.02	234 MPa		
0.04	248 MPa		

Table 3: The material properties of woven carbon fiber/epoxy composites [Qrimli, Mahdi and Ismail (2015); Performance Composites (2009)]

Young's modulus		Shear modulus		Poisson ratio		Density
E_x (GPa)	67	G_{xy} (GPa)	5.31	ν_{xy}	0.26	
E_y (GPa)	67	G_{yz} (GPa)	3.07	ν_{yz}	0.26	1600 kg/m^3
E_z (GPa)	5.6	G_{xz} (GPa)	3.07	ν_{xz}	0.26	

The finite element models of PCB were built with the above-mentioned dimensions and material properties. The solid-shell element SOLSH190, adopted for modeling the PCB structures, has eight nodes and three degree of freedom for each node in the x, y, z directions. In this paper, the applied load, normal to the PCB, for dynamic analysis was given to simulate a shock test [Integrated Service Technology (2019)]. The support excitation scheme was used in the finite element analysis, so the four screw holes in the PCB were fixed as boundary condition [Yeh and Lai (2006); MIL-STD-883E (1997)]. Fig. 4 shows the finite element model of the PCB and boundary condition.

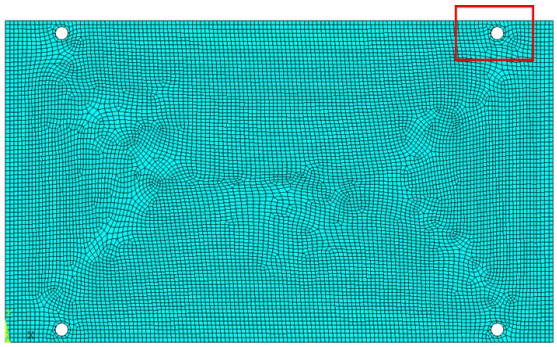

(a) Finite element model of PCB

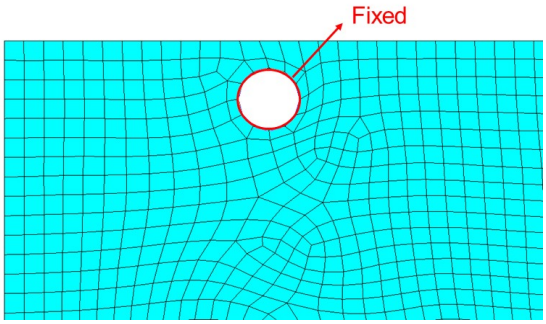

(b) Boundary condition of PCB

Figure 4: Finite element model of PCB and boundary condition

The acceleration load with a peak 1500 g and pulse duration 0.5 ms was applied on all nodes, normal to the PCB, as a shock loading in the finite element model according to the standard Mil-Std-883E Method [MIL-STD-883E (1997); Yin, Peng, Kayani et al. (2016)], as shown in Fig. 5. After being applied by a shock loading, the deformation and stress distribution of PCB were analyzed.

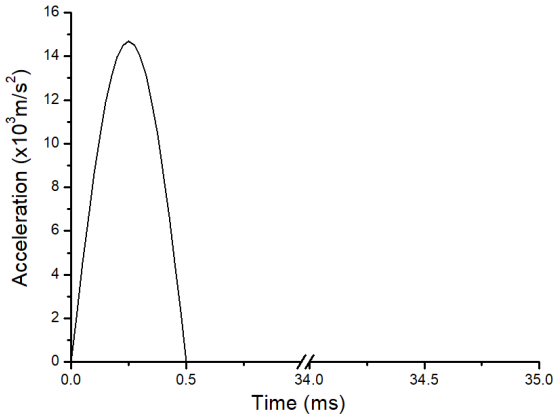

Figure 5: Acceleration load *vs.* time

2.2 Convergence analysis

In order to ensure the accuracy of simulation, the convergence of the finite element model of PCB was analyzed first. The maximum von Mises stress in E-glass/epoxy layer for finite element models of the PCB with different element numbers under the shock loading was obtained, as shown in Tab. 4. When the element number of the analysis model of PCB is over 11,527, the difference of the maximum von Mises stress is under 2%, as shown in Fig. 6. Therefore, the finite element model of the PCB with 11,527 elements was adopted for the subsequent analyses. Fig. 4(a) shows the meshed finite element model with 11,527 elements.

Table 4: The maximum von Mises stress for finite element models with different element numbers

Node number	Element number	Maximum von Mises stress	Difference
3922	1864	313 MPa	17.8%
6048	2906	326 MPa	14.4%
10,544	5,119	335 MPa	12.1%
23,512	11,527	375 MPa	1.5%
85,424	42,271	381 MPa	-

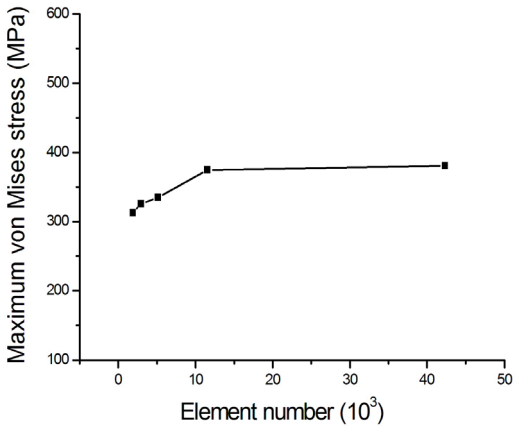

Figure 6: The maximum von Mises stress versus element number of finite element model

3 Results and discussion

The results of the finite element analysis are discussed in three parts. At first, the deformation and stress distribution of the standard 8-layer PCB under the shock loading were analyzed. Then, the deformation and stress distribution of the PCB with different thickness were evaluated. The failure of PCB was assessed based on the stress states in each ingredient material and ignored the possibility of interfacial failure. Lastly, the finite

element model of the PCB with a lower strength was selected to change the composite material from E-glass/epoxy to carbon fiber/epoxy for discussion of strength enhancement.

3.1 The standard PCB under shock loading

3.1.1 The deformation of standard PCB under shock loading

Large deformation of PCB might induce failure of interconnection between the chip and the PCB, or the failure of PCB and chip. This study focused on the deformation at the central region of the PCB since the chips were located at the central region of PCB generally. Moreover, the deformation of PCB during the shock loading was contributed by the out-of-plane displacement in the direction of shock loading in the finite element analysis. Fig. 7(a) shows the out-of-plane displacement variation at the central region of PCB under the shock loading from the finite element analysis. The maximum out-of-plane displacement of PCB occurred at 1.98 ms during the shock loading and the deformation of PCB is shown in Fig. 7(b).

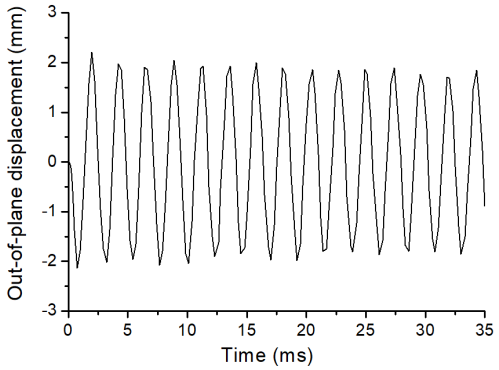

(a) The displacement variation at the central region of PCB under shock loading

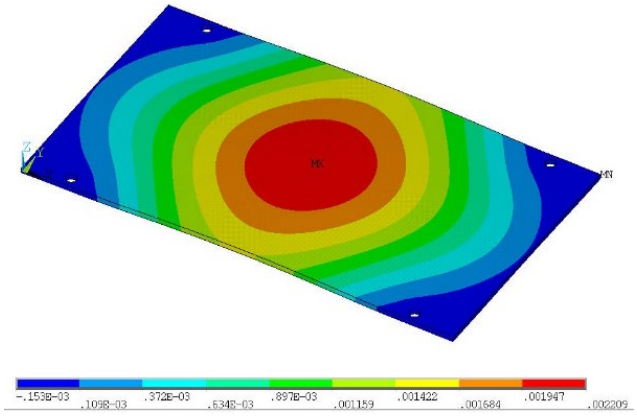

(b) The deformation of PCB at 1.98 ms

Figure 7: The displacement and deformaiton of PCB

3.1.2 The stress distribution of standard PCB under shock loading

In addition to the deformation of PCB, the von Mises stress variation of the PCB under the shock loading from the finite element analysis was obtained, as shown in Fig. 8. The maximum von Mises stress at 1.98 ms, which occurred at the maximum out-of-plane displacement of PCB, is 195.5 MPa. Since this stress level is much lower than the failure strength of copper foil, 318 MPa [Yin, Peng, Kayani et al. (2016)], the failure of PCB may not happen by the shock loading. It is consistent with the practical operation in industry. The maximum principal stress of each layer at the central cross section of PCB was extracted and plotted, as shown in Fig. 9. The results show that the principal stress distribution is symmetric about the middle plane of the cross section of PCB and the principal stress increases from inner to outer part of PCB. The highest principal stress in E-glass/epoxy occurred at the top and bottom layers of PCB.

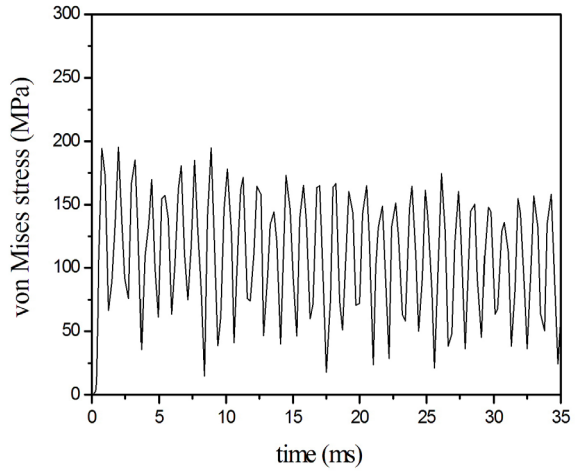

Figure 8: The von Mises stress variation in top copper layer at the central region of PCB under shock loading

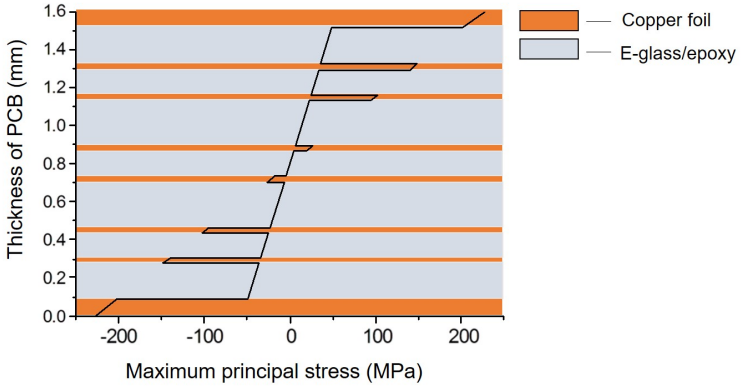

Figure 9: The maximum principal stress in each layer at the central region of PCB

3.2 The PCB with different thickness under shock loading

The deformation and stress distribution of the PCB with different number of layers under the shock loading were investigated by the finite element analysis to understand the correlation between the thickness of PCB and stress level under the shock loading. The PCBs with a thickness ranging from 0.6 mm to 2.6 mm according to stacked layers are discussed. The number of copper foil layer and composite layer in the PCBs with different thickness is summarized in Tab. 5. Fig. 10 shows the maximum von Mises stress of the top-layer copper foil in the PCBs with different thickness by the finite element analysis. The maximum von Mises stress of top copper foil layer decreases 5% when the thickness of PCBs increases from 0.6 mm to 2.6 mm.

Table 5: The number of copper foil layer and core layer in PCBs with different thickness

Total thickness of PCB (mm)	0.6	1.0	1.6	2.2	2.6
Number of copper foil layer	4	6	9	12	14
Number of core layer	3	5	8	11	13
Total number of layers	7	11	17	23	27

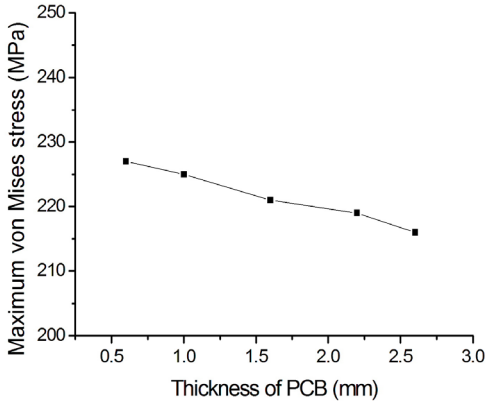

Figure 10: The maximum von Mises stress of top copper foil layer in PCBs with different thickness

The deformation and principal stress of the PCB with 2.6 mm thickness under the shock loading at 1.98 ms are discussed. Since the maximum deformation occurs at the central region of PCB, as shown in Fig. 11, and the electronic devices are practically located around the central region of PCB, this study focused on the principal stress distribution in core layer 1 at the central region of PCB, as shown in Fig. 12.

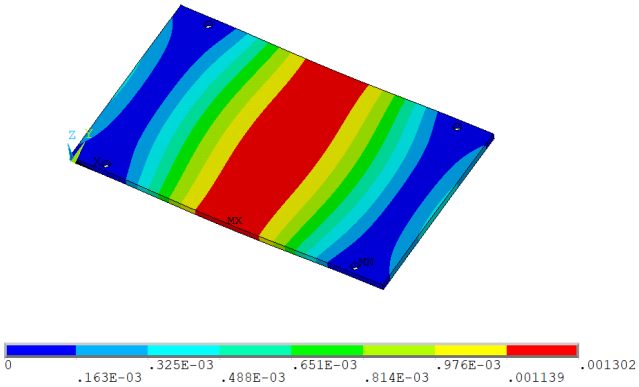

Figure 11: The deformation of 2.6 mm PCB under shock loading at 1.98 ms

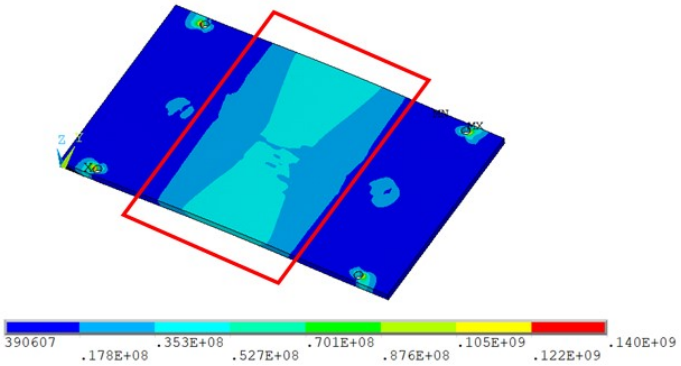

(a) The principal stress distribution in the core layer 1 of PCB

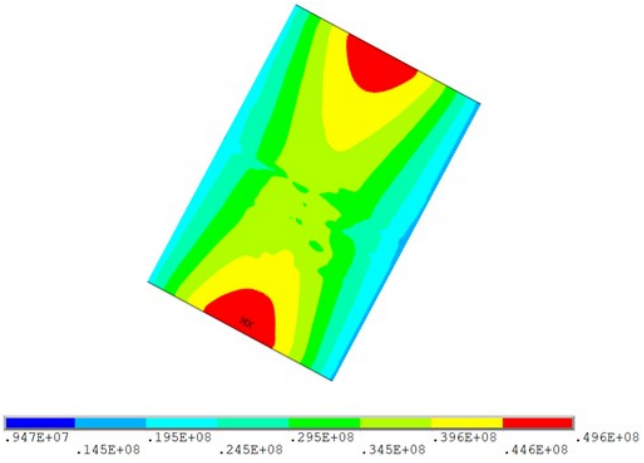

(b) The principal stress distribution in core layer 1 at the central region of PCB

Figure 12: The principal stress distribution of 2.6 mm PCB under shock loading at 1.98 ms

According to the results of the finite element analysis, the PCB with 2.6 mm thickness has the lowest stress under the shock loading. Failure strength of materials, including copper foil, woven E-glass/epoxy, and woven carbon fiber/epoxy, are shown in Tab. 6 [Tan, Tong and Steven (2001); Qrimli, Mahdi and Ismail (2015); Yin, Peng, Kayani et al. (2016)]. The maximum principal stress of E-glass/epoxy layer in the PCB with 2.6 mm thickness under the shock loading by the finite element analysis is 49.6 MPa and is smaller than its failure strength 587 MPa.

Table 6: The failure strength of copper foil, woven E-glass/epoxy, and woven carbon fiber/epoxy [Tan, Tong and Steven (2001); Qrimli, Mahdi and Ismail (2015); Yin, Peng, Kayani et al. (2016)]

Material	Copper foil	Woven E-glass/epoxy	Woven carbon fiber/epoxy
Failure strength	318 MPa	587 MPa	894 MPa

3.3 The PCB with different composite materials under shock loading

The maximum von Mises stress of copper foil of the PCB with 0.6 mm thickness under the shock loading 1500 g by the finie element analysis is higer than those in the PCBs with different thickness. To improve the strength of the PCB with 0.6 mm thickness, the thinner and weaker one, the woven E-glass/epoxy core layer of PCB was replaced by woven carbon fiber/epoxy composites. The finite element results are summarized in Tab. 7.

Table 7: The results for PCB with 0.6 mm thickness and different composite materials for core layer under shock loading 1500 g

Materials of core layers	E-glass/epoxy	Carbon fiber/epoxy	Difference
Maximum displacement of PCB	2.665 mm	2.276 mm	-14.6%
Maximum principal stress in core layer at the central region of PCB	49.9 MPa	82.3 MPa	64.9%
Maximum von Mises stress in copper foil layer at the central region of PCB	136 MPa	127 MPa	-6.6%

The maximum displacement of PCB decreases 14.6%, when using carbon fiber/epoxy as the core layer. A smaller deformation was obtained since the PCB with carbon fiber/epoxy under the shock loading had a higher stiffness. Furthermore, the maximum von Mises stress in copper foil at the central region of PCB reduced 6.6% by adopting the carbon fiber/epoxy as the core layer in PCB. The carbon fiber/epoxy shared a part of stress with copper foil during the shock loading. Although the maximum principal stress

in the core layer of PCB increased around 64.9% at the central region of PCB by using carbon fiber/epoxy, the stress is still under its failure strength. The results indicate that the PCB with carbon fiber/epoxy has a higher strength and a lower possibility for the failure of PCB than that with E-glass/epoxy.

3.4 The PCB under higher level shock loading

For harsh operating conditions, such as those used in the automotive industry and military, the acceleration peak during the shock loading is higher than the condition used for portable devices. Referring to the standard MIL-STD-883 Method [MIL-STD-883E (1997)], the finite element model of the PCB with 2.6 mm, the thicker and stronger one, is subjected to a shock loading with a peak value of 5000 g and 0.3 ms for pulse duration.

The results show that the stresses in both copper foil layer and core layer increase significantly in the PCB with carbon fiber/epoxy as core layer, as shown in Tab. 8. However, the stress levels for both core layer and copper foil are still lower than the failure strengths of carbon fiber/epoxy and copper foil. These results show the integrity of the PCB structure with 2.6 mm thickness, under 5000 g shock loading, when using carbon fiber/epoxy as the core layer.

Table 8: Comparison of the finite element results for the PCB with 2.6 mm thickness under 1500 g and 5000 g shock loading

Materials of core layers	E-glass /epoxy	Carbon fiber/epoxy
Shock loading	1500 g	5000 g
Maximum principal stress in core layer at the central region of PCB	49.6 MPa	220 MPa
Maximum von Mises stress in copper foil layer at the central region of PCB	147 MPa	170 MPa

4 Conclusions

This study evaluated the deformation and stress of the PCB with different thickness and composite materials under the shock loading by the finite element analysis. The possibility of failure for the PCB under the shock loading was discussed by comparing the finite element results and the failure strength of materials used in analysis. The summary is as follows.

(1) The maximum out-of-plane displacement and von Mises stress of the standard PCB occurred at 1.98 ms and the stress level is lower than the failure strength of woven E-glass/epoxy under the shock loading 1500 g. Moreover, a higher principal stress located in copper foil at the top and bottom layer of PCB.

(2) For the PCB with different thickness, the thicker PCB (2.6 mm) could reduce the maximum von Mises of copper foil in PCB around 5% than that for the thinner PCB

(0.6 mm).

(3) Adopting the carbon fiber/epoxy as the core layer material instead of E-glass/epoxy could reduce the stress of copper foil around 6.6%.

(4) For the applications in harsh environment, the maximum stresses of fiber/epoxy core layer and copper foil in the PCB with 2.6 mm thickness under the shock loading 5000 g are smaller than their corresponding failure strengths.

Acknowledgement: The authors greatly thank the support from Ministry of Science and Technology, Taiwan, R. O. C., through grant MOST-105-2221-E-007-031-MY3.

Conflicts of Interest: The authors declare that they have no conflicts of interest to report regarding the present study.

References

ANSYS (2019): Engineering simulation & 3D design software. https://www.ansys.com/.

Ebnesajjad, S. (2013): *Polyvinyl Fluoride*. William Andrew.

Grout, I. (2008): *Digital Systems Design with FPGAs and CPLDs*. Elsevier.

Hanafi, J.; Jobiliong, E.; Christiani, A.; Soenarta, D. C.; Kurniawan, J. et al. (2012): Material recovery and characterization of PCB from electronic waste. *Procedia-Social and Behavioral Sciences*, vol. 57, no. 9, pp. 331-338.

Iannuzzelli, R. (1991): Predicting plated-through-hole reliability in high temperature manufacturing processes. *IEEE Electronic Components and Technology Conference*, pp. 410-421.

Integrated Service Technology (2019): Mechanical shock test.

https://www.istgroup.com/tw/service/mechanical-shock-test.

JESD22 B111 (2003): Board level drop test method of components for handheld electronic products. *JEDEC Standard*.

Jie, G.; Lim, C. T.; Tay, A. A. O. (2004): Modeling of solder joint failure due to PCB bending during drop impact. *Proceedings of 6th Electronics Packaging Technology Conference*, pp. 678-683.

MatWeb (2019): Copper, Cu, annealed.

http://www.matweb.com/search/DataSheet.aspx?MatGUID=9aebe83845c04c1db5126fada6f76f7e.

MIL-STD-883E (1997): Test method standard for microcircuits. http://scipp.ucsc.edu/groups/fermi/electronics/mil-std-883.pdf.

Nanotech Elektronik (2019): Materials for printed circuit boards. http://www.nanotech-elektronik.pl/index.php/en/info/materials.

Ong, Y. C.; Shim, V. P. W.; Chai, T. C.; Lim, C. T. (2003): Comparison of mechanical response of PCBs subjected to product-level and board-level drop impact tests. *Proceedings of the 5th Electronics Packaging Technology Conference*, pp. 223-227.

Qrimli, H. F. A.; Mahdi, F. A.; Ismail, F. B. (2015): Carbon/Epoxy woven composite experimental and numerical simulation to predict tensile performance. *Advances in Materials Science and Applications*, vol. 4, no. 2, pp. 33-41.

Pcbcart (2019): Layer stackup.

https://www.pcbcart.com/pcb-capability/layer-stackup.html.

Performance Composites (2009): Mechanical properties of Carbon fibre composite materials, fibre/Epoxy resin (120°C cure).

http://www.performance-composites.com/carbonfibre/mechanicalproperties_2.asp.

Rahman, A. S.; Rangari, V.; Jeelani, S. (2015): Thermal and mechanical properties of woven glass fiber reinforced Epoxy composites with Carbon nanotubes grown in-situ. *International Journal of Engineering and Science*, vol. 4, no. 12, pp. 54-61.

Reiff, D.; Bradley, E. (2005): A novel mechanical shock test method to evaluate lead-free BGA solder joint reliability. *Proceedings Electronic Components and Technology*, vol. 2, pp. 1519-1525.

Tan, P.; Tong, L.; Steven, G. P. (2001): Mechanical behavior for 3-D orthogonal woven E-glass/Epoxy composites. *Journal of Reinforced Plastics and Composites*, vol. 20, no. 4, pp. 274-303.

Tummala, R. R. (2001): *Fundamentals of Microsystems Packaging*. McGraw-Hill.

Wang, K. Y. (2012): *Development and Application of Composite Material Lamination Theory for Printed Circuit Boards (Master's Thesis)*. Auburn University, Alabama.

Wang, Y.; Low, K. H.; Pang, H. L. J.; Hoon, K. H.; Che, F. X. et al. (2006): Modeling and simulation for a drop-impact analysis of multi-layered printed circuit boards. *Microelectronics Reliability*, vol. 46, no. 2-4, pp. 558-573.

Wang, Y. Q.; Low, K. H.; Che, F. X.; Pang, H. L. J.; Yeo, S. P. (2003): Modeling and simulation of printed circuit board drop test. *Proceedings of the 5th Electronics Packaging Technology Conference*, pp. 263-268.

Wong, E. H.; Lim, K. M.; Lee, N.; Seah, S.; Hoe, C. et al. (2002): Drop impact test-mechanics & physics of failure. *4th Electronics Packaging Technology Conference*, pp. 327-2395.

Yeh, C. L.; Lai, Y. S. (2006): Support excitation scheme for transient analysis of JEDEC board-level drop test. *Microelectronics Reliability*, vol. 46, no. 2-4, pp. 626-636.

Yin, X. Q.; Peng, L. J.; Kayani, S.; Cheng, L. J.; Wang, W. et al. (2016): Mechanical properties and microstructure of rolled and electrodeposited thin copper foil. *Rare Metals*, vol. 35, no. 12, pp. 909-914.

Zhang, B.; Ding, H.; Sheng, X. (2009): Reliability study of board-level lead-free interconnections under sequential thermal cycling and drop impact. *Microelectronics Reliability*, vol. 49, no. 5, pp. 530-536.

Zhang, H. W.; Liu, Y.; Wang, J.; Sun, F. L. (2015): Effect of elevated temperature on PCB responses and solder interconnect reliability under vibration loading. *Microelectronics Reliability*, vol. 55, no. 11, pp. 2391-2395.